Towards Computing Ratcheting and Training in Superconducting Magnets

P. Ferracin, S. Caspi, and A. F. Lietzke

***Abstract*—The Superconducting Magnet Group at Lawrence Berkeley National Laboratory (LBNL) has been developing 3D finite element models to predict the behavior of high field Nb_3Sn superconducting magnets. The models track the coil response during assembly, cool-down, and excitation, with particular interest on displacements when frictional forces arise. As Lorentz forces were cycled, irreversible displacements were computed and compared with strain gauge measurements. Additional analysis was done on the local frictional energy released during magnet excitation, and the resulting temperature rise. Magnet quenching and training was correlated to the level of energy release during such mechanical displacements under frictional forces. We report in this paper the computational results of the ratcheting process, the impact of friction, and the path-dependent energy release leading to a computed magnet training curve.**

***Index Terms*—Ratcheting, superconducting magnet, training.**

I. Introduction

In a superconducting magnet, quenching occurs when a superconducting cable undergoes a transition to the normal resistive state [1]. A quench may happen either because the superconductor reaches its short sample limit, or because of transient disturbances like flux jumping or mechanical motions which locally heat the cable above the quench temperature [2], [3]. Mechanical disturbances are driven by large Lorentz forces acting on the winding during excitation. Under such forces, a superconducting cable may move with respect to the surrounding structure, at the same time producing cracks in the epoxy impregnation. Both events result in a release of energy that may trigger a quench [4].

Another phenomenon typical to superconducting magnets is training, i.e. the progressive improvement of quench current after repeated quenching. This process can be explained by assuming that, after a quench induced by a mechanical motion, the coil is partially locked by friction in a new and more secure stress condition. On subsequent current ramps, this condition allows the coil to withstand higher levels of Lorentz forces.

In past years, significant effort has been devoted by the Superconducting Magnet Group at LBNL towards the study of the quenching processes in superconducting magnet. This effort has been focused in two main directions. On one side, a detailed analysis of the voltage signal recorded right before and after a quench has been performed, with the goal of investigating the causes (flux-jumps or stick-slip mechanical motions) and the locations of the quench [5]. On the other side, 3D finite element models have been implemented to study coil movements during excitation, with the goal of contributing to the interpretation of magnet performances, and, ultimately, to improve training [6]. We present in this paper an attempt to simulate and reproduce a magnet training behavior through a finite element model. In particular, the model investigates the progressive change in coil shape forced by consecutive current ramps, and the energy released by a frictional movement of a conductor. As a preliminary model validation, we compare the computations with the test results of SQ02, a subscale racetrack quadrupole magnet recently fabricated and tested as part of the LARP Program [7].

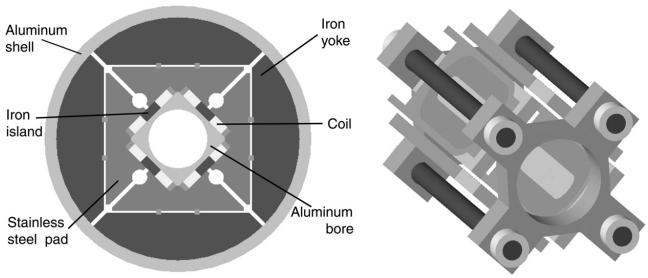

Fig. 1. SQ01 magnet cross-section (left) and longitudinal support (right).

II. Subscale Quadrupole Magnet (SQ02)

A. Design Features and Training Performance

The design of the subscale quadrupole magnet SQ02 (Fig. 1) consists of four subscale coil modules, about 300 mm long. Each coil module is wound around an aluminum-bronze pole (island) in a flat racetrack double-layer configuration. After winding, the coils are reacted, epoxy impregnated, and placed around a square aluminum bore. According to short sample measurements, the SQ02 expected current limit is 9.9 kA at 4.3 K, with a peak field of 11.1 T located in the pole turn. The support structure, described in details in [8], comprises of stainless steel pads, iron yokes, and an aluminum outer shell. The room-temperature pre-loading of the structure is obtained through pressurized bladders inserted between yokes and pads. During cool-down, the shell generates further pre-load on the coils, due to the different thermal contractions of aluminum and iron. A system of four aluminum rods and a stainless steel plate is included in the design to support axially the coils. Both shell and aluminum rods are instrumented with strain gauges.

The test of SQ02 included two thermal cycles at 4.3 K (we refer to [9] for a complete description of the test results). The magnet had a first quench at 5.9 kA (60% of I_{ss}), and it reached

Manuscript received August 26, 2006. This work was supported by the Director, Office of Energy Research, Office of High Energy and Nuclear Physics, High Energy Physics Division, U.S. Department of Energy under Contract DE-AC02-05CH11231.

The authors are with the Lawrence Berkeley National Lab, Berkeley, CA 94720 USA (e-mail: pferracin@lbl.gov).

Digital Object Identifier 10.1109/TASC.2007.898515

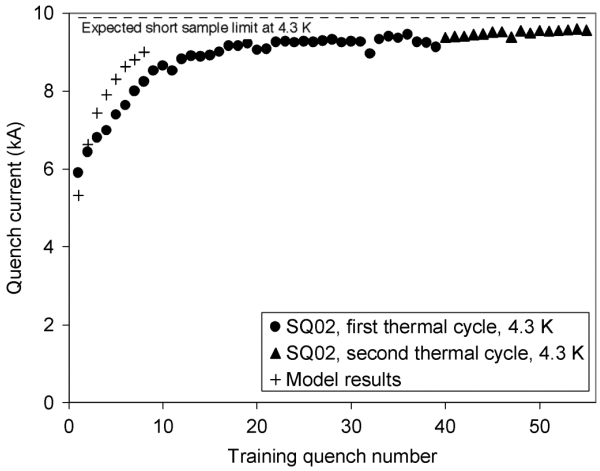

Fig. 2. Training performance of SQ02 at 4.3 K (two thermal cycles). The dashed line represents the expected current limits based on short sample measurements. The cross markers represent the results of the FE model.

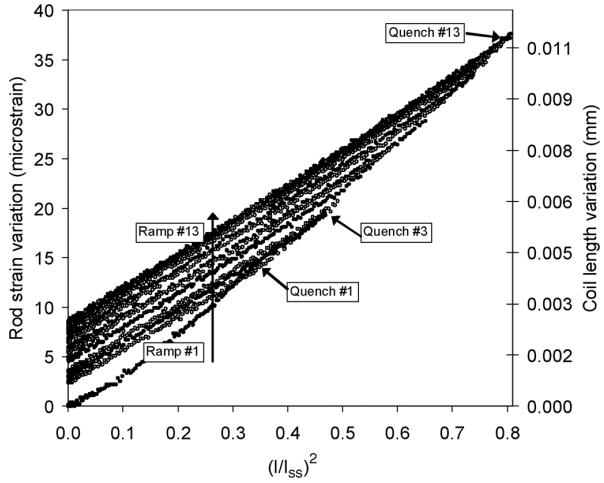

Fig. 3. Measured variation of rod strain (left axis) and length (right axis) as a function of the Lorentz force.

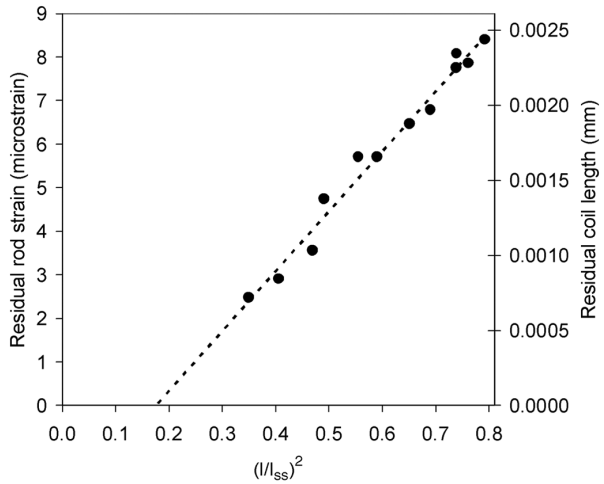

Fig. 4. Measured residual rod strain (left axis) and rod elongation (right axis) as a function of the Lorentz force reached during an excitation cycle.

the maximum quench current of 9.5 kA (97% of I_{ss}) in the second thermal cycle. As shown in Fig. 2 (the figure includes results of the finite element model that will be discussed in the following sections), two different regimes characterized the training curve: in the first 13 quenches, the magnet rapidly reached about 90% of I_{ss}, with an average increase of 200 A to 400 A between consecutive quenches. In subsequent ramps, the quench current increased at a significantly lower rate, approaching almost asymptotically the maximum current. All the training quenches were located in the innermost turn around the island (pole turn), were the highest field was expected. A series of voltage taps, distributed between the inner and outer layer of the pole turn, enabled us to perform a detailed analysis of the quench locations. The analysis indicated that the training quenches originated in the end region, and progressively moved towards the center of the straight section. Then, as the magnet reached its maximum current, all the quench locations reversed back to the end region (close to the tip of the island), where the coil peak field is located. We will show in the next sections that part of this behavior can be reproduced by the finite element model.

B. Strain Gauge Measurements

The coil mechanical behavior during excitation was recorded with strain gauges mounted on axial aluminum rods. Since the rods were in direct contact with the coil ends (via end plates), any change in rod strain corresponded to a coil axial displacement. During the first 13 quenches, when most of the magnet training occurred, the continuous measuring of the rod strain clearly showed the on going deformation process. In Fig. 3, the incremental increase in rod strain (and coil length) is plotted as a function of the fraction of Lorentz force with respect to the 4.3 K short sample value ($(I/I_{ss})^2$). The axial component of the Lorentz force tends to pull the coil-end outwardly, thus axially stretching the rods. Prior to the first quench, the rods stretch 15 μstrain, corresponding to a total coil elongation of about 4 μm. After the quench, when the current reduces to zero and the Lorentz force vanishes, the rods maintain a residual strain (about 3 μstrain), indicating that the coil remains partially elongated. During subsequent training ramps, as the current reaches higher levels, the residual strain increases as well, indicating that the larger the force, the longer the coil (Fig. 4). This phenomenon, called ratcheting, has been already observed in previous magnets [10]–[13], and can be related to the friction between the components, which, after a quench, locks the coil in a new position, and prevents it from returning to its original place.

III. Finite Element Model

A. General features and goals

A complete 3D finite element analysis of SQ02 has been performed in order to interpret the test results (see Fig. 5(a)). The model simulates the coil mechanical behavior during all its phases from magnet assembly to operation, and allows for coil separation from the island. Friction has been applied to the contact elements between island and coil (Figs. 5(b) and 5(c)). The goal of the study was to understand and reproduce the main features described in the previous section: the occurrence of quenches in the pole turn, the progressive axial elongation of the coil (ratcheting), and the increase in quench current during the test (training). With respect to previous analyses [6], this study

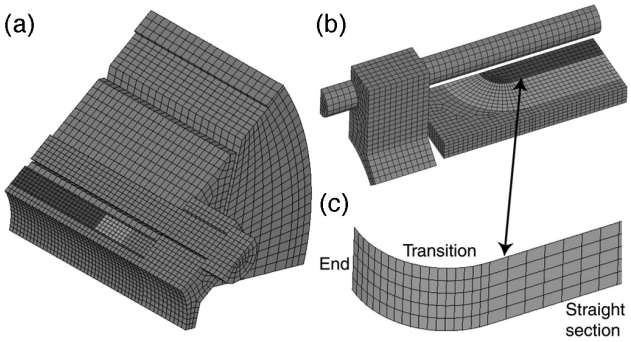

Fig. 5. Finite element model of the SQ02 geometry (a), with details of the coil end support (b), and of the contact region between coil and island (c).

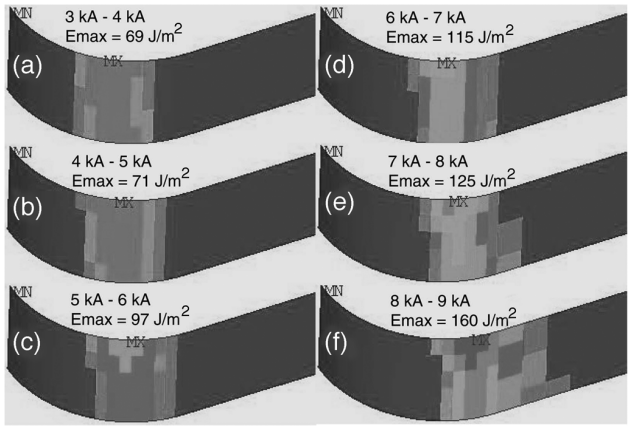

Fig. 6. Frictional energy $(\mathrm{J/m^2})$ dissipated during excitation from 3 kA to 9 kA in steps of 1 kA. $\mathrm{E_{max}}$ is the peak frictional energy dissipated in one step.

added the frictional energy dissipated due to conductor motion. Moreover, we performed a series of computations that included consecutive current cycles of loading and unloading, and combined the dissipated energy with a thermal model, in an attempt to find out the temperature increase and to reproduce qualitatively a training curve.

B. Frictional Energy Dissipation

Let's assume a friction factor μ between coil and island. During excitation, Lorentz forces elongate the coil, causing a relative sliding δ (m) of the pole turn with respect to the island. Opposing frictional forces are proportional to the frictional stress $\sigma_{\|}(\mathrm{N/m^2})$ between the coil and the island. The combined frictional force and sliding result in an energy dissipation (per unit area) that can be calculated as $\delta \cdot \sigma_{\|}(\mathrm{J/m^2})$.

We computed the frictional energy dissipation during excitation, assuming a friction factor between coil and island of 0.5 (best fit of SQ02 experimental data). The results, plotted in Fig. 6, show that, from 3 kA to 4 kA, the release of frictional energy near the end peaks at about 69 $\mathrm{J/m^2}$. During the following current steps, the dissipated energy progressively increases to a maximum of 160 $\mathrm{J/m^2}$, and its location gradually moves towards the straight section (confirming the quench location pattern observed during magnet test). As shown in Fig. 7, the energy dissipation during a current ramp varies linearly with the Lorentz force, and its maximum depends on the friction factor used in the model.

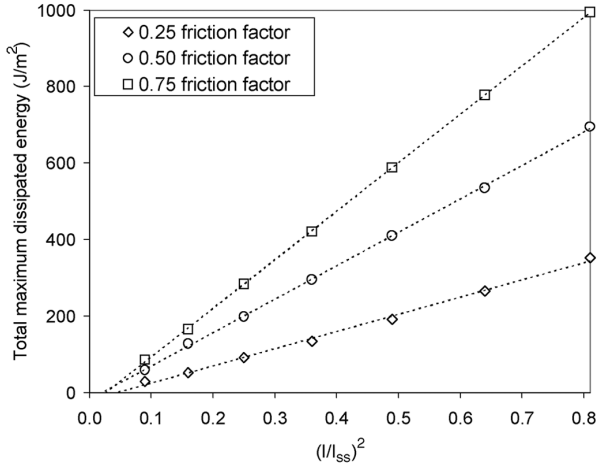

Fig. 7. Computed total frictional energy dissipated during a current ramp.

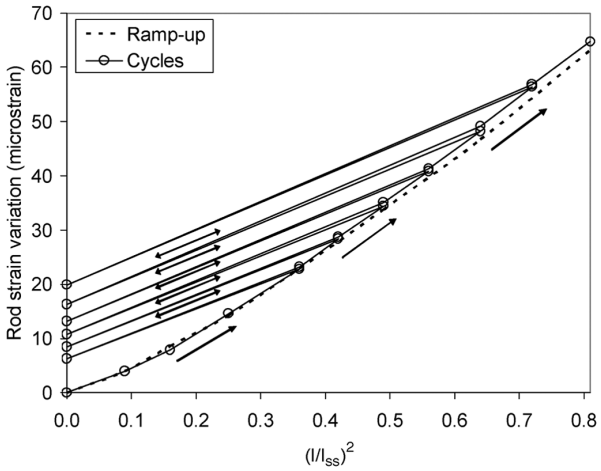

Fig. 8. Computed variation of rod strain as a function of the Lorentz force.

C. Ratcheting Model

In order to model the coil ratcheting, we performed two different computations (see Fig. 8). In the first computation we increased continuously the Lorentz forces ("ramp-up" case). In the second computation ("cycles" case), we firstly introduced a load cycle where the force is initially raised, and then abruptly removed. Then, on subsequent cycles, we repeat the process by reapplying the Lorentz force, first to its previous value, and then to a new higher current. It appears that, when friction is included and loads are cycled, the simulation becomes non-conservative, and the results are path-dependent. The computed rod strain, under zero Lorentz force condition, is now continuously changing (ratcheting) with respect to previous load cycles. By doing so it is possible to reproduce the irreversible deformation (residual elongation) that a coil experiences when the forces are removed. It is clear that once the same forces are re-applied, the coil returns to its previous deformed state, and when the current is further increased, the coil experiences "virgin-territory", with an increase in strain along the "ramp-up" curve.

As shown in Fig. 9, the same path-dependent behavior is observed for the frictional energy. Imagine that the coil is sliding during "ramp-up": the maximum energy released in the 6.0 kA–6.5 kA current range is about 56 $\mathrm{J/m^2}$ (Fig. 9(a)).

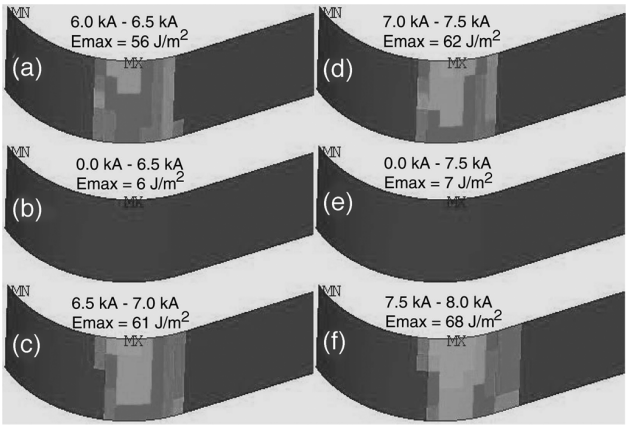

Fig. 9. Frictional energy $(\mathrm{J/m^2})$ dissipated by cycled current ramps. $\mathrm{E_{max}}$ is the peak of frictional energy dissipated in one step.

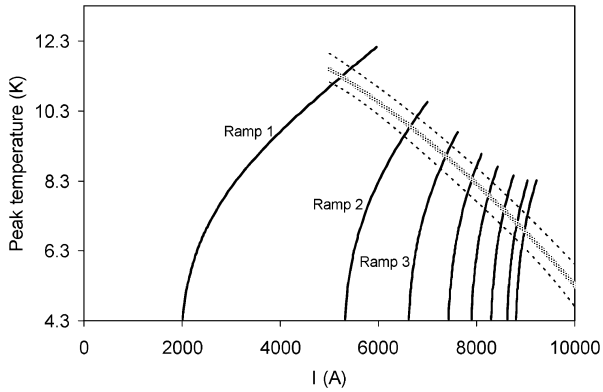

Fig. 10. Peak temperature of the superconductor induced by frictional energy computed during consecutive current ramps (solid black lines). The gray line represents the temperature of current sharing vs. current.

Assuming that a quench occurs at 6.5 kA, we first remove the force, and then ramp again varying the current from 0 kA to 6.5 kA (Fig. 9(b)). The energy dissipated during this second ramp is practically negligible (with a maximum of 6 $\mathrm{J/m^2}$). When the current is further increased from 6.5 kA–7.0 kA (Fig. 9(c)), the coil tracks the "ramp-up" curve again, and the energy reaches a peak of 61 $\mathrm{J/m^2}$. This analysis, repeated in Figs. 9(d), 9(e), and 9(f), proves that after a quench, the frictional model predicts a new state of deformation for the coil, which minimizes the dissipated energy until the coil experiences a new level of forces (virgin territory).

D. Training Model

As a final step in the analysis, the energy computed in the mechanical model (Fig. 7) has been implemented into a simplified 2D finite element adiabatic model. The model includes the superconducting strands, the cable-island insulation, and the aluminum-bronze island. Adiabatic conditions are imposed at the boundaries of the model, and no heat transfer is considered longitudinally. The heat source is obtained by the conversion of the frictional energy $(\mathrm{J/m^2})$, computed by the 3D mechanical model, in a heat pulse $(\mathrm{J/m^3/s})$: assuming that all the frictional energy accumulated during a given ramp is released in 1 ms (typical duration of a quench triggering event [5]), the resulting temperature rise in the superconductor can be computed (Fig. 10, solid black line), and compared with the temperature of current sharing (gray line). For example, during the first current ramp, the energy dissipated from 0 kA to 5.3 kA raises the temperature of superconductor to its current sharing temperature of 11.3 K. In this condition, a quench is expected, and the current is brought to zero. During the second ramp, as a result of the path-dependent behavior, a negligible amount of energy is dissipated up to the previous quench current. Then, the model predicts that the conductor temperature of current sharing is reached at a current of 6.6 kA. By repeating the computation with increasing currents, and decreasing temperature margin, a computed training curve can be generated, which reproduces qualitatively the training observed in SQ02 (see Fig. 2).

IV. Conclusion

The present analysis indicates that it is possible to reproduce non-reversible processes, like ratcheting and training, observed in superconducting magnet. When friction is include in a finite element model, the estimated coil deformations and frictional energies exhibit a significant path-dependent behavior. Combining a mechanical model with a thermal model, one can therefore reproduce a series of consecutive quenches at progressively higher current. This new analysis may provide useful insight on magnet performances and on the effect of different coil stress conditions on training.

References

[1] M. N. Wilson, *Superconducting Magnets*. Oxford: Clarendon Press, 1983, ch. 5.

[2] A. Devred, "Quench origins," in *AIP Conf. Proc.*, 1992, vol. 249, p. 1263.

[3] S. L. Wipf, Stability and Degradation of Superconducting Current-Carrying Devices Los Alamos Report, LA 7275, 1978.

[4] M. N. Wilson and R. Wolf, "Calculation of minimum quench energies for Ritherford cables," *IEEE Trans. Appl. Supercond.*, vol. 7, no. 2, pp. 950–953, June 1997.

[5] A. F. Lietzke *et al.*, "Differentiation of performance-limiting voltage transients during $\mathrm{Nb_3Sn}$ magnet testing," in *AIP Conf. Proc.*, 2006, vol. 824, p. 550.

[6] S. Caspi *et al.*, "Towards integrated design and modeling of high field accelerator magnets," *IEEE Trans. Appl. Supercond.*, vol. 16, no. 2, pp. 1298–1303, June 2006.

[7] S. A. Gourlay *et al.*, "Magnet R&D for the US LHC accelerator research program," *IEEE Trans. Appl. Supercond.*, vol. 16, no. 2, pp. 324–327, June 2006.

[8] P. Ferracin *et al.*, "Development of a large aperture $\mathrm{Nb_3Sn}$ racetrack quadrupole magnet," *IEEE Trans. Appl. Supercond.*, vol. 15, no. 2, pp. 1132–1135, June 2005.

[9] P. Ferracin *et al.*, "Assembly and test of SQ02, a $\mathrm{Nb_3Sn}$ racetrack quadrupole magnet for LARP," presented at the Applied Superconductivity Conference 2006, Seattle, WA, USA, August 29–September 1 2006, unpublished.

[10] J. Strait *et al.*, "Tests of full scale SSC R&D dipole magnets," *IEEE Trans. Magn.*, vol. 25, no. 2, pp. 1455–1458, March 1989.

[11] J. Buckley *et al.*, "Mechanical performance of a twin-aperture 56 mm bore 1 m long dipole model made with SSC type cables," *IEEE Trans. Magn.*, vol. 32, no. 4, pp. 2136–2139, July 1996.

[12] A. Devred *et al.*, "About the mechanics of SSC dipole magnet prototypes," in *AIP Conf. Proc.*, 1992, vol. 249, p. 1309.

[13] S. Mattafirri *et al.*, "Performance analysis of HD1: A 16 T $\mathrm{Nb_3Sn}$ dipole magnet," *IEEE Trans. Appl. Supercond.*, vol. 15, no. 2, pp. 1156–1159, June 2005.